JOURNAL OF SOLID STATE CHEMISTRY 90, 102–108 (1991)

Structure of Amorphous $Ta_2O_5 \cdot nH_2O$ Derived from Peroxo-Polytantalate Solution

A. KISHIMOTO, H. SUGIMOTO,* T. NANBA,† AND T. KUDO

*Institute of Industrial Science University of Tokyo, Roppongi 7-22-1, Minato-ku, Tokyo, Japan 106; * Faculty of Engineering, Science University of Tokyo, Kagurazaka, 1-3, Shinjyuku-ku, Tokyo, Japan 162*

Received July 11, 1990; in revised form September 18, 1990

The structure of tantalum oxide hydrate derived from peroxo poly-tantalate was investigated on the basis of XRD analyses. The peak positions in the pair distribution functions (PDF) for as-prepared and postannealed samples correspond with those calculated from the crystalline L-Ta_2O_5. Microcluster models for each sample were constructed and the validities of these models were confirmed by comparison between their calculated PDFs and their observed ones. © 1991 Academic Press, Inc.

Introduction

One of the authors found that a kind of peroxo-polytungstic acid (W-IPA) was synthesized by the direct reaction of metallic W with H_2O_2 and was isolated as an amorphous glassy matter (*1*). W-IPA is spin-coatable on various substrates and thin films thus formed are applicable to an inorganic resist material because of its photosensitivity. Heat-treated films of W-IPA ($WO_3 \cdot nH_2O$) exhibit electrochromism as reversible as that of evaporated WO_3 films (*2*). The amorphous structure of W-IPA and $WO_3 \cdot nH_2O$ derived from its heat-treatment have been investigated by XRD analyses.

Recently we found that a kind of polytantalate anion (Ta-IPA) analogous to that of W-IPA is formed by the reaction of $Ta(OC_2O_5)_5$ with H_2O_2 (aqueous solutions), and that thin films fabricated by spin-coating of that solution exhibit significant ionic conductivity due probably to migration of H^+ within the amorphous matrix of $Ta_2O_5 \cdot nH_2O$ (*3*). To elucidate the scheme of proton conduction, however, structural information about the matrix is essential.

In this paper we report the results of the XRD structural analysis performed with bulk $Ta_2O_5 \cdot nH_2O$ formed from the tantalate solution. The structures of the films could be approximated from that of the bulk matrix.

Experimental

Preparation of peroxo-polytantalic acid was similar to that reported (*3*). Ethanol-diluted tantalum ethoxide $Ta(OC_2O_5)_5$ was slowly added to H_2O_2/C_2H_5OH solution. A small amount of white matter precipitated but it quickly dissolved, giving an almost clear solution. Ethanol was evaporated at

† Present address: Faculty of Engineering, Okayama University, Tsushima naka 3-1-1, Okayama, Japan

0022-4596/91 $3.00

room temperature. The solution was then transferred to a separatory funnel together with diethyl ether to remove organic compounds produced during the reaction. The residual ether was evaporated and excess H_2O_2 was decomposed catalytically with platinum black. After removing the small amount of undissolved impurities by filtration, the solution yielded a clear peroxo-polytantalic acid (Ta-IPA) solution. As the Ta-IPA solution was dried by blown air, it turned into a gel phase when the concentration of Ta-IPA exceeded a certain value (ca. 0.33 mol/liter: Ta atom mole per 1 liter of solution). Further drying gave rise to a spherical white solid 1 to 3 mm in diameter. Powder specimens were obtained by grinding with an agate mortar.

Thermogravimetric (TG) and differential thermal analysis (DTA) were conducted using a Simadzu DT-40. Density was measured by a pycnometer using benzene as measuring liquid. XRD measurement was carried out with a step-scanning method for 300 ~ 600 sec of fixed counting time. A Mo$K\alpha$ radiation with an output of 60 kV–150 mA was monochromatized with Zr–Y-balanced filters, a graphite monochromator in a diffracted beam, and a pulse height analyzer. Pair distribution function (PDF) was obtained by an ordinary method (*4*).

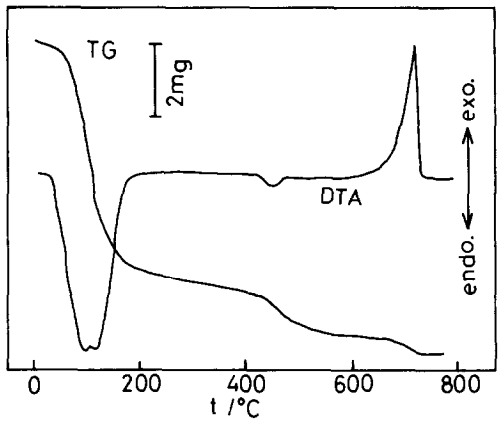

FIG. 1. Thermogravimetric (TG) and differential thermal analysis (DTA) for Ta-IPA powder. (Initial weight, 45.7 mg; heating rate, 20°C/min; atmosphere, dry N_2.)

Results

Figure 1 shows the TG-DTA result recorded with tantalum oxide hydrate derived from peroxo-polytantalate. This material undergoes a three-step thermal decomposition. There are two plateaus around 350 and 520°C, which were confirmed to be stable states because no weight change was observed after the specimen was kept at these two temperatures. The amounts of water in the annealed sample at 340°C for 30 min and at 510°C for 30 min were calculated to be 1.7 and 0.2 per 1 mole Ta_2O_5, respectively. The value for the as-prepared specimen was about 6.5, which depended slightly on preparation conditions or ambient humidity.

There are two DT endothermic peaks around 150 and 430°C, both accompanied by a loss in weight. The former is probably due to the release of water molecules of zeolitic nature, and the latter is of a structural nature. At higher temperatures around 650°C, the peroxo-polytantalate shows a strong DT exothermic peak, which is due to crystallization heat. This crystalline phase obtained by annealing at 710°C (10 min) was confirmed to be orthorhombic (a = 6.198, b = 40.290, c = 3.888 Å, Z = 11) tantalum which is a δ phase as reported in Refs. (*6*, *7*). The samples annealed below 340°C showed only halo peaks in XRD. Some small crystalline peaks were seen in the XRD of the 510°C annealed sample. But crystallization was not completed when the heat treatment temperature was lower than 530°C, because the halo peak was predominant in the XRD of the specimen treated at 530°C for 2 hr.

Structural analyses using PDF were carried out for two plateau stages and the as-

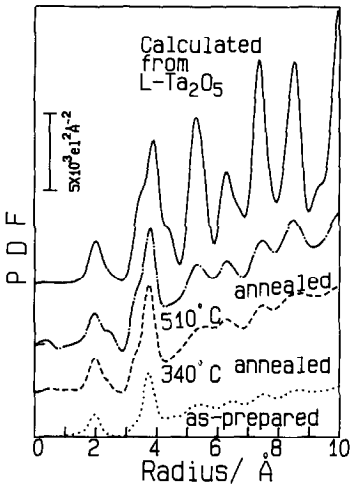

FIG. 2. Observed PDFs for as-prepared and postannealed Ta-IPA Dotted line, as-prepared sample; dashed line, 340°C/30 min annealed sample; dash-dotted line, 510°C/30 min annealed sample. (The PDF calculated from L-Ta_2O_5 (solid line) is shown for comparison.)

prepared one. The observed PDFs are shown in Fig. 2, in which the calculated PDF from the crystalline L-Ta_2O_5 is also shown for comparison. Two main peaks can be observed at about 2 and 4 Å, which may be attributed to the nearest neighbors of Ta–O and Ta–Ta, respectively. Peaks seen above 4 Å are located at almost the same position for every sample.

A small peak or shoulder is commonly seen at 3.4 Å adjacent to the second peak. This peak can be assigned to a shorter Ta–Ta. Therefore in any sample there are two nearest Ta–Ta distances, mainly 3.8 Å and a shorter one of ~3.4 Å.

The average coordination numbers of the nearest Ta–Ta pairs (Nco) were obtained from the second peaks. First, deconvolution of the overlapping second peak was performed by means of the pair function method and the ratio of Nco (short)/Nco (total) [Nco (total) = Nco (long) + Nco (short)] was estimated. Then the total Nco were calculated. These are listed in Table I together with other data. It can be seen that the higher the annealing temperature, the larger the Nco (total) and the ratio of Nco (short).

Discussion

Structural Model

Previously we performed PDF structural analysis of amorphous W-IPA assuming a cluster-micro void model. Observed PDF were well explained on such a model and estimated structures were supported by spectroscopical data. Specimens of the present study also showed a halo peak in the small diffraction angle region, suggest-

TABLE I

THE AMOUNT OF WATER (n), DENSITY, AND COORDINATION NUMBER (Nco) OF THE NEAREST Ta–Ta FOR AS-PREPARED AND POSTANNEALED SAMPLES

	As-prepared	340°C/30 min	510°C/30 min	710°C/30 min
n	6.5	1.7	0.2	0
Density (g cm^{-3})	3.6	5.9	6.1	8.2
Nco				
Long (3.8 Å)	4	4.5	4.5	—
Short (3.4 Å)	1	1.5	1.8	—
Total	5	6	6.3	*(8)*[a]

[a] Estimated from the crystal structure.

ing they were composed of clusters. These facts lead us to a similar cluster model.

As has already been shown in Fig. 2, observed PDFs for each sample resemble that calculated from crystalline L-Ta_2O_5. The crystal structure of L-Ta_2O_5 is represented by a sheet arrangement along the c-axis of corner-shared TaO_7 (pentagonal bipyramid) and TaO_6 (octahedron) coordination polyhedra, and very complicated in the a–b plane, in which there are, on the average, three distortion planes along the long b-axis. Except for the vicinity of distortion planes, however, the a–b plane is composed of a structural unit as shown in Fig. 3a. Thus it is reasonable to construct cluster models based on such a unit because only rather short-range atomic arrangements are in question for the present case, though this is not meant to exclude the possible existence of other structural models which may also explain the observed data.

The actual unit used for our model construction is a slightly modified arrangement as shown by the solid line in Fig. 3b. This unit can be expanded in the a–b plane without distortion, resulting finally in a infinite network of the pg plane group in the rectangular system (shown by the dashed line in the figure) in which Ta atoms are located at $2a(x, 0)$ and $2a(\frac{1}{2}, \frac{1}{4})$. Referring to the Ta coordinates in Fig. 3(a), the rectangular cell dimensions (a, b) and the positional parameter x may be approximated as (6.89, 7.24) and 0.308, respectively.

Four distinct Ta–Ta distances thus occur in the a–b plane, but these are classified into two groups, the average Ta–Ta distance for longer and shorter groups being 3.8 and 3.4 Å. It is noted that the Ta–Ta distance along c-axis (perpendicular to the plane) is almost the same as the longer distance. The shoulder seen in the PDF main peak reflects such a situation.

Consequently the problem is primarily reduced to constructing an n-fold columnar cluster consisting of fragment sheets appro-

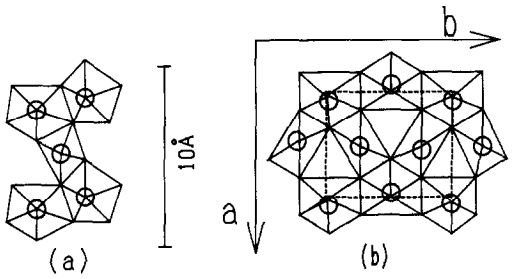

FIG. 3. (a) Crystal structure of L-Ta_2O_5 (without distortion). (b) The unit used for model construction. (Coordination polyhedral model, projected to the a–b plane; circle, Ta.)

priately cut off from the a–b plane that it satisfies the observed Nco and Nco(short)/Nco(total) at the same time.

The Nco increases with an increase in both horizontal size and layer number (n). However, the shorter length Ta–Ta distance (3.4 Å) exists only in the a–b plane not along the c-axis Ta. Therefore the Nco(short)/Nco(total) decreases with increasing layer number (n) if the planar shape remains constant.

Model for the As-Prepared Sample

For example, four-layered cluster model shown in Fig. 4c was constructed for the as-prepared sample. Model construction procedures will be described briefly.

Each Ta in the a–b plane is surrounded by six Ta atoms. Locating a TaO_6 octahedron at the center, it is surrounded by two edge sharing TaO_7 pentagonal bipyramids, two corner sharing TaO_7 pentagonal bipyramids, and two octahedra (Fig. 4a, solid line).

First, a fourfold cluster consisting of such a sheet was selected as a starting model. Compared with the observed Nco (5.0), the calculated Nco from this model was rather small (4.9). If one more TaO_6 or TaO_7 polyhedron is added to the initial cluster (Fig. 4a), the average coordination number (Nco) increases and Nco = 5.0 is real-

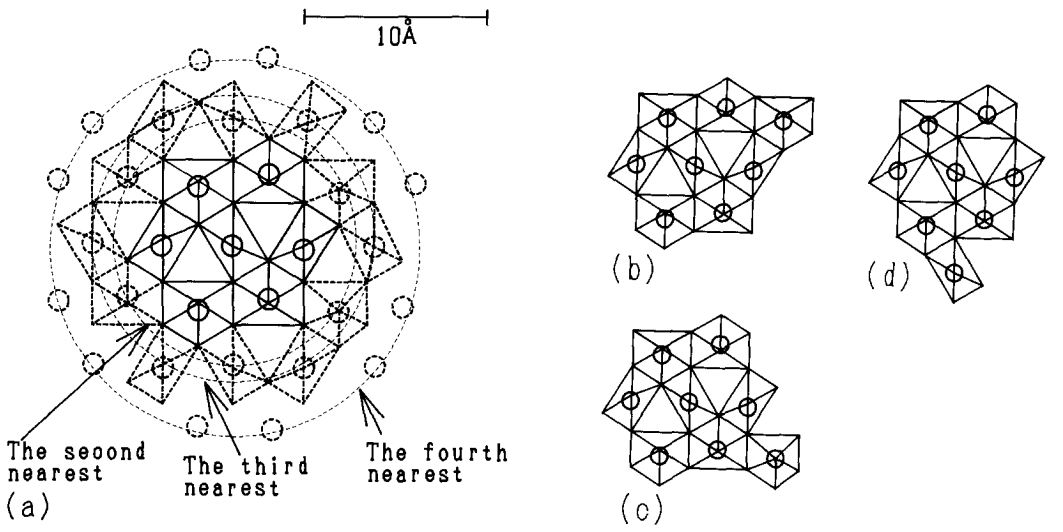

FIG. 4. (a) Initial structural model (solid line) for as-prepared sample; 2nd-, 3rd-, and 4th-nearest Ta atom from the central octahedra are also illustrated (dashed line) (projected to the a–b plane; circle, Ta; layer number = 4). (b, c, d) Modified structural model for as-prepared sample. (All are larger than the initial model by one polyhedra.)

ized. However, there are three types of candidate clusters as shown in Fig. 4 (b), (c) and (d). We selected cluster model (c) because the calculated Nco(short)/Nco(total) from this modified model is $\frac{1}{5}$, which is very close to the observed one.

The calculated PDF from this cluster model is shown in Fig. 5. It shows good agreement with the observed value up to the second peak. The profile over that peak is also closely correlated but the electron density of the calculated PDF is smaller than that of the observed one. This is probably because we did not consider the contribution of the atomic pairs between the clusters.

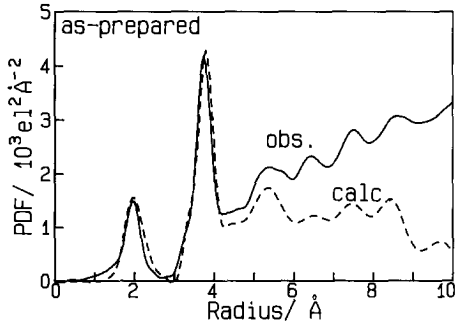

FIG. 5. Comparison between model PDF (dashed line) and observed PDF (solid line) for as-prepared sample.

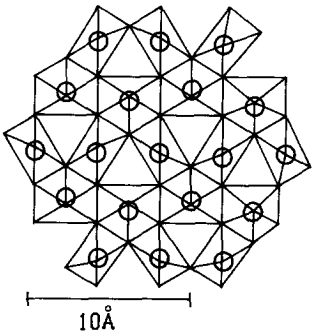

FIG. 6. Structural model for 340°C/30 min annealed sample. (Projected to a–b plane; circle, Ta; layer number = 4.)

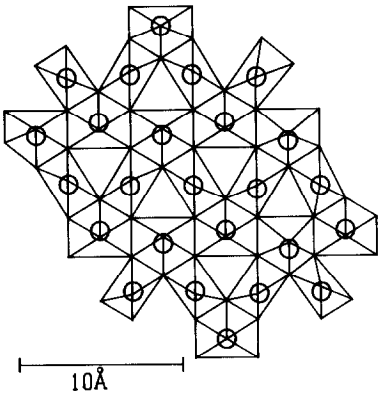

FIG. 7. Structural model for 510°C/30 min annealed sample. (Projected to a–b plane; circle, Ta; layer number = 8.)

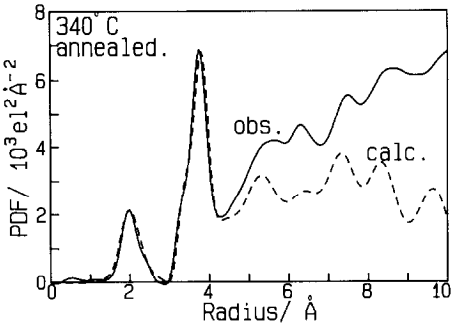

FIG. 8. Comparison between model PDF (dashed line) and observed PDF (solid line) for 340°C/30 min annealed sample.

Models for Heat-Treated Samples

Similarly constructed models for 340°C- and 510°C-annealed samples are shown in Figs. 6 and 7. The calculated PDFs are consistent with the observed ones, which are shown in Figs. 8 and 9.

The model for the 340°C-annealed sample is composed of the second and third nearest polyhedra in addition to the as-prepared one. There are six second nearest and six third nearest polyhedral sites as shown in Fig. 4a (dotted line). When we add all polyhedra to the as-prepared model (Fig. 6), the calculated Nco and the ratio of Nco(short) fit satisfactorily with the observed ones. In other words, the cluster growth during the heat treatment may be rather isotropic.

On the other hand, heat treatment at a higher temperature (510°C) caused further cluster growth, but the growth was somewhat anisotropic. The outermost twelve dotted circles in Fig. 4a represent the fourth nearest Ta atoms from the center Ta. A considerably large value of the Nco(short)/Nco(total) (1/3.5) observed with 510°C-treated sample was realized by selecting only six Ta atoms having the shorter Ta–Ta distance between the third nearest Ta atoms and adding their polyhedra to Fig. 7. The eight-layered cluster model gave a calculated PDF in very good agreement with the observed one, as shown in Fig. 9.

TABLE II

NEAREST COORDINATION NUMBER FOR SAMPLES AND MODELS

	As-preapred	340°C/30 min	510°C/30 min
Nco (total)			
Observed	5.0	6.0	6.3
Model	5.0	5.92	6.23
Ratio of Nco (short)			
Observed	1/5.0	1/4.0	1/3.5
Model	1/5.0	1/4.1	1/3.54

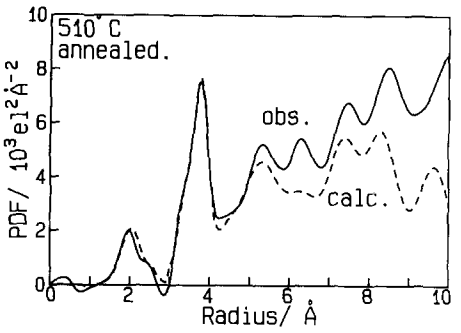

FIG. 9. Comparison between model PDF (dashed line) and observed PDF (solid line) for 510°C/30 min annealed sample.

The observed and model clusters' Nco and ratio of short Ta–Ta distance among the total are summarized in Table II. It can be concluded that the amorphous structure of solid Ta–IPA consists of columnar cluster in which the basic network structure of crystalline Ta_2O_5 is maintained in the amorphous state.

References

1. T. KUDO, *Nature (London)* **312,** 537 (1984).
2. K. YAMANAKA, H. OKAMOTO, H. KIDOU, AND T. KUDO, *Japan. J. Appl. Phys.* **25,** 1420 (1986).
3. A. KISHIMOTO, T. NANBA, AND T. KUDO, *Solid State Ionics,* to be published.
4. T. NANBA AND I. YASUI, *J. Solid State Chem.*, **83,** 304 (1989).
5. N. C. STEPHENSON AND R. S. ROTH, *Acta Crystallogr.* **B27,** 1037 (1971).
6. K. LEHOVEC, *J. Less-Common Metals* **7,** 397 (1964).
7. N. TERAO, *Japan. J. Appl. Phys.*, **6,** 21 (1967).